P3.49 An Analysis of Total Lightning Over North Alabama During the 2 March 2012 Tornado Event

Brian C. Carcione
National Weather Service, Huntsville, AL

Kristopher D. White
NWS/NASA Short-term Prediction Research and Transition (SPoRT) Center, Huntsville, AL

Geoffrey T. Stano
NASA SPoRT/ENSCO, Inc., Huntsville, AL

1. Introduction

The 2 March 2012 tornado outbreak is best-known for its violent tornadoes across the Ohio Valley. However, the first tornadoes of the day occurred farther to the south in northern Alabama. Two significant tornadoes occurred in just over one hour: a long-track EF-3 from 1510 to 1600 UTC, and a shorter EF-2 from 1610 to 1615 UTC. (Another brief, weak tornado occurred 1608 to 1610 UTC.) An additional round of severe weather occurred later in the afternoon, beginning around 1955 UTC. The second round of storms was characterized more by large hail (including reports of hail as large as baseballs and softballs) than tornadoes, though four additional weak (EF-0 and EF-1) and brief tornadoes occurred between 1955 and 2146 UTC. Figure 1 shows all of the tornado tracks for the day over northern Alabama and southern Tennessee.

The morning portion of the event over northern Alabama was generally more favorable for tornadogenesis, characterized by higher low-level wind shear and lower lifting condensation level (LCL) heights compared to the afternoon. Figure 2a and 2b illustrate RUC proximity soundings from 1600 UTC, during the most active part of the morning event, and 2000 UTC, during the most active part of the afternoon event. Surface-based CAPE decreased slightly (1841 J kg^{-1} to 1502 J kg^{-1}) but 0-3 km storm-relative helicity decreased from 508 $m^2 s^{-2}$ to 342 $m^2 s^{-2}$, and the LCL height increased from 875 m to 1225 m. While the afternoon values were clearly still favorable for tornadoes, it appears that there were fewer (if any) low-level boundaries in place to facilitate or enhance tornadogenesis (Markowski 1998).

Data from the North Alabama Lightning Mapping Array (NALMA) were used in real-time operations during the event, especially during the morning tornadoes (White et al. 2012). The NALMA is a very high frequency (VHF) detection network (Koshak et al. 2004, Goodman et al. 2005) consisting of 11 sensors spread across northern Alabama and two sensors located in the Atlanta, GA, region. The primary advantage of this network is that it detects total lightning, or the combination of both cloud-to-ground and intra-cloud lightning, instead of cloud-to-ground lightning alone. This helps to build a complete picture of storm evolution and development, and can serve as a proxy for storm updraft strength (Williams et. al. 1999, Goodman et. al. 2005), particularly since intra-cloud lightning makes up the majority of all lightning in a typical thunderstorm.

While the NALMA data do not directly indicate severe weather, they can indirectly indicate when a storm is strengthening (weakening) due to increases (decreases) in updraft strength, as the updraft is responsible for charging mechanisms within the storm. Data output are VHF radiation sources, which are produced during lightning breakdown processes. These sources are processed into 2x2 km source density grids (hereafter simplified to “sources”) and are ported into the Advanced Weather Interactive Processing System (AWIPS) for National Weather Service (NWS) offices in Huntsville, AL, Nashville, TN, Morristown, TN, and Birmingham, AL, in near real-time. These data are produced at sub-radar volume scan temporal updates every two minutes. An increase in source density correlates to increased lightning activity and trends in updraft magnitude as long as the storm is within about 240 km of the center of the network.

Operationally, these data have been used at the Huntsville Weather Forecast Office (WFO) since early 2003 through collaborations with the NASA Short-term Prediction Research and Transition Center (SPoRT; Darden et. al. 2002, Goodman et al. 2004). Over nearly ten years of operational use, these total lightning observations have become an essential tool for forecasters during real-time warning operations (Bridenstine et. al. 2005, Nadler et al. 2009, Darden et. al. 2010, Stano et al. 2011, White et al. 2012). One of the operational advantages of the NALMA is the two-minute temporal resolution of the data, providing forecasters with two to three updates during a typical volume scan of the WSR-88D radar. The total lightning data can increase a forecaster's confidence to issue or not issue a warning, since the NALMA data provide additional insight into the storm's evolution between radar volume scans.

2. NALMA USE FOR WARNING DECISION-MAKING

As previously mentioned, NALMA data were particularly useful for operational warning decision-making during the morning thunderstorms. During the initial phases of the event, it was clear that storms were beginning to rotate and slowly intensify, but radar data were not particularly illuminating otherwise. At 1444 UTC, a line of showers and thunderstorms was aligned from southwest to northeast across Lawrence and Limestone counties. 0.5-degree radar reflectivity values were between 60 and 65 dBZ near the towns of Oliver and Red Bank and maximum sources were just over 200, indicating the areas of heaviest rainfall and strongest updraft, respectively. A broad area of cyclonic rotation and moderately low Correlation Coefficient (CC or ρ_{hv}) values also were evident in northern Lawrence County. The KHTX 3.4-degree elevation scan (corresponding to temperatures around -20°C in this area and elevation of 7.3 km AGL) indicated maximum reflectivity values around 55 dBZ, which is near generally-accepted empirical values for severe hail. While data suggested that hail was present in the storm, the lack of a deep core of relatively high reflectivities and only moderately low CC values indicated that the hail diameter was not likely at 2.5 cm or greater (e.g. criteria for a severe thunderstorm warning).

With radar data not yet suggesting severe hail was present, and with no severe weather reports from nearby storm spotters, a warning was not issued at 1444 UTC. However, numerical model guidance and mesoscale analyses suggested the storm was moving into a more favorable environment for storm organization, and strengthening was considered possible. The NALMA data from 1446 UTC made it clear that the storm was indeed strengthening. A sudden increase in sources was noted (Figure 3, upper left), with maximum densities climbing to over 400 sources. This was an increase of greater than 200 percent in just two minutes, and more than three times the running standard deviation from the previous 10 minutes. Roughly applied to the thresholds from Schultz et al. (2009), this lightning "jump" likely indicated severe weather was imminent because it represented a significant increase in updraft strength.

With this new information in mind and other radar data (e.g., relatively high reflectivity, and moderately low CC values) approaching the thresholds for severe weather, the first severe warning of that morning was issued at 1451 UTC. At 1505 UTC, the first severe weather report of quarter size (2.5 cm) hail was received at WFO Huntsville. As the storm moved downstream, hail the size of golf balls (4.4 cm) and a wind gust estimated at 31 m s^{-1} was reported by local law enforcement at 1512 UTC.

The NALMA sources increased rapidly before the onset of severe weather, including hail, and then decreased before the tornado developed, which matches most conceptual models offered in earlier research (e.g., Williams et al. 1999). These data aided in the warning decision-making process and increased lead time of the initial severe thunderstorm warning.

3. MORNING SIGNIFICANT TORNADOES

The original supercell that prompted the severe thunderstorm warning at 1451 UTC also produced a long-track tornado shortly thereafter. The tornado touched down in the Canebrake community just south of Athens in Limestone County. It began at 1510 UTC, and continued along a 54.8 km path through Limestone and Madison Counties, producing peak winds of 63 m s^{-1} (EF-3 on the Enhanced Fujita Scale).

As discussed, there was a pronounced increase in sources prior to the tornado touchdown. However, total lightning often becomes an afterthought when radar and satellite are sufficient, or when the workload demands of a tornado on the ground do not permit interrogation of additional data. It begs the question: can total lightning provide additional useful information about a tornado in real time?

To that end, total lightning source density values for the long-track EF-3 tornado were plotted versus time (Figure 4). There is a prolonged lightning jump from 1536 to 1544 UTC, increasing more than sixteen times the 10-min running standard deviation. The jump preceded the most intense portion of the tornado path across northeastern Madison County, AL, by approximately 6 minutes. Around the same time, a second lobe of NALMA sources developed and exhibited a jump in its own right (200 to 400 sources at 1546 UTC). The subsequent decreases in both lobes correspond to a general weakening trend, and the tornado lifted at 1600 UTC.

Similar trends were observed with the second significant tornado of the morning, an EF-2 that touched down barely 10 minutes after the first had lifted, but lasted a much shorter time. Figure 5 displays the same total lightning temporal trend; much like the first tornado, the second tornado reaches a relative intensity maximum at the same time as sources reached a peak. Additional research on long-track tornadoes is planned to determine if this trend is common, or dependent on storm or environment.

4. AFTERNOON WEAK TORNADOES AND LARGE HAIL

A second wave of severe thunderstorms occurred during the afternoon of 2 March, beginning at 1955 UTC. Low-level wind shear decreased while deep-layer shear remained robust, resulting in a transition to damaging winds and large hail. The majority of the severe weather reports occurred after 1900 UTC, including all of the “giant” hail (> 5 cm) reports. Four weak (EF-0 or EF-1) tornadoes were also reported, all of which occurred within a 24 km radius. Three of the four tornadoes and all of the giant hail reports occurred with just two supercells, which will be analyzed here.

The first supercell developed across Colbert and Lawrence counties around 1930 UTC. A significant jump in sources (greater than 4 standard deviations) occurred at 1944 UTC, and the first tornado of the afternoon, an EF-0, followed at 1955 UTC in northwestern Limestone County, AL. The total lightning trend followed the expected conceptual model, with the tornado occurring well after the initial jump and as the sources fell sharply. Quarter-size hail was also reported with the supercell at 2000 UTC.

Subsequent hail reports associated with this supercell were all preceded by sharp increases, if not full two-standard deviation lightning jumps as suggested by Schultz et al. (2009). There is some difficulty in determining whether jumps preceded severe weather since there were multiple source increase/decrease combinations during the life cycle of the storm. However, it is worth noting that sources dropped off markedly by 2030 UTC, as the supercell moved into southern Tennessee. Sources exceeded 20 just once after that time, yet the storm continued to produce large hail to the size of baseballs as it moved into southeastern Tennessee. This problem is most likely due to degraded detection efficiency of the NALMA network, which suffered damage during the 27 April 2011 outbreak and was operating with 6 sensors centered on the Huntsville area, instead of the normal 11. The network has since been restored to full capability as of Spring 2012.

A second supercell developed over extreme northeastern Mississippi and crossed the Alabama border around 2000 UTC. In short order, it produced quarter-size hail (2007 UTC), baseball-size hail (2015 UTC), and softball-size hail (2035 UTC) across Colbert and Lauderdale counties. NALMA data are comparatively unimpressive during this span, exceeding 20 sources just four times. Some type of increase preceded two of the three hail reports, but they are not large enough to be called jumps and could easily be dismissed as noise by operational meteorologists in the heart of an event. The small values and subtle increases can likely be attributed to the degraded state of the network, since source density products are more susceptible to network degradation compared to flash density products. SPoRT will transition to providing flash density products to partner WFOs in the future as the AWIPS II software is implemented within the NWS.

A more robust increase—more than three standard deviations—preceded an EF-0 tornado in Limestone County by just two minutes. Another increase occurred eight minutes later and preceded an EF-1 tornado in Limestone County by 6 minutes. Both of these increases occurred as the storm moved into the heart of the NALMA network, increasing the likelihood that total lightning would be properly detected.

In general, afternoon storms were characterized by smaller source density values than the morning storms, and consequently increases were much more subtle and difficult to detect. The largest jumps occurred as the storms entered the heart of the NALMA networks, but these jumps corresponded well to severe weather reports and tornadoes.

5. SUMMARY AND FUTURE WORK

Total lightning information from the North Alabama Lightning Mapping Array was highly beneficial to operational meteorologists at WFO Huntsville during the morning of 2 March 2012. A pronounced lightning jump alerted the warning forecaster that a seemingly-marginal severe thunderstorm was more likely to produce severe weather, providing increased lead time over the use of Doppler radar alone. However, diminished detection efficiency hurt the utility of the data in real time during the afternoon despite the continuing severe weather threat.

The launch of GOES-R in 2015 will help eliminate such detection efficiency issues while bringing total lightning detection to a much larger domain (Figure 6). The Geostationary Lightning Mapper (GLM) instrument will provide total lightning to almost a full-disk domain, but at a lower spatial resolution than existing ground-based networks (10 km at nadir versus 1 km or 2 km).

Additional tools are also under development to help alert forecasters to lightning jumps. A tool jointly developed by WFO Huntsville and SPoRT will provide real-time trending information as a time series (example in Figure 7) so that forecasters can visualize trends more easily. This makes total lightning more relevant and useful in a time-sensitive operational environment. In addition, the NWS is funding a project to automate the lightning jump detection outlined by Schultz et al. (2009). The automated lightning jump algorithm would eliminate the need to interrogate the raw total lighting information, expediting the warning decision-making process while and increasing forecaster confidence and warning lead time.

6. REFERENCES

Bridenstine, P., C. B. Darden, J. Burks, S. J. Goodman, 2005: The Application of Total Lightning Data in the Warning Decision Making Process, Preprints *Conference on the Meteorological Applications of Lightning Data*, San Diego, CA, January 2005.

Darden, C., B. Carroll, S. Goodman, G. Jedlovec, B. Lapenta, 2002: Bridging the gap between research and operations in the National Weather Service: Collaborative activities among the Huntsville meteorological community. NOAA Tech. Memo. NWS SR-222. [Available online at www.srh.noaa.gov/ssd/techmemo/sr222.pdf.]

Darden, C. B., D. J. Nadler, B. C. Carcione, R. J. Blakeslee, G. T. Stano, D. E. Buechler, 2010: Utilitizing Total Lightning Information to Diagnose Convective Trends. *Bull. Amer. Meteor. Soc.*, **91**, 167-175.

Goodman, S. J. and Coauthors, 2005: The North Alabama lightning mapping array: Recent severe storm observations and future prospects. *Atmos. Res.*, **76**, 423–437.

Koshak, W. J., and Coauthors 2004: North Alabama Lightning Mapping Array (LMA): VHF source retrieval algorithm and error analysis. *J. Atmos. Oceanic Technol.*, **21**, 543-558.

Markowski, P. M., J. M. Straka, E. N. Rasmussen, D. O. Blanchard, 1998: Variability of Storm-Relative Helicity during VORTEX. *Mon. Wea. Rev.*, **126**, 2959–2971.

Nadler, D. J., C. B. Darden, G. T. Stano, and D. E. Buechler, 2009: An operational perspective of total lighting information. *4th Conf. on the Meteorological Applications of Lightning Data*, Amer. Meteor. Soc., Phoenix, AZ, P1.11.

Schultz, C. J., W. A. Petersen, and L. D. Carey, 2009: Preliminary development and evaluation of lightning jump algorithms for the real-time detection of severe weather. *J. Appl. Meteor. Climatol.*, **48**, 2543-2563.

Stano, G. T., K. K. Fuell, and G. J. Jedlovec, 2011: Improved real-time lightning trend products. 5th *Conf. on Meteorological Applications of Lightning Data*, Amer. Meteor. Soc., Seattle, WA, 23-27 Jan 11, 8.1., 8pp.

Williams, E., and Coauthors, 1999: The behavior of total lightning activity in severe Florida Thunderstorms. *Atmos. Res.*, **51**, 245–265.

White, K., B. Carcione, C. J. Schultz, G. T. Stano, and L. D. Carey, 2012: The use of the North Alabama Lightning Mapping Array in the real-time operational warning environment during the March 2, 2012 severe weather outbreak in Northern Alabama. *NWA Newsletter*, Oct. 2012, No. 12-10.

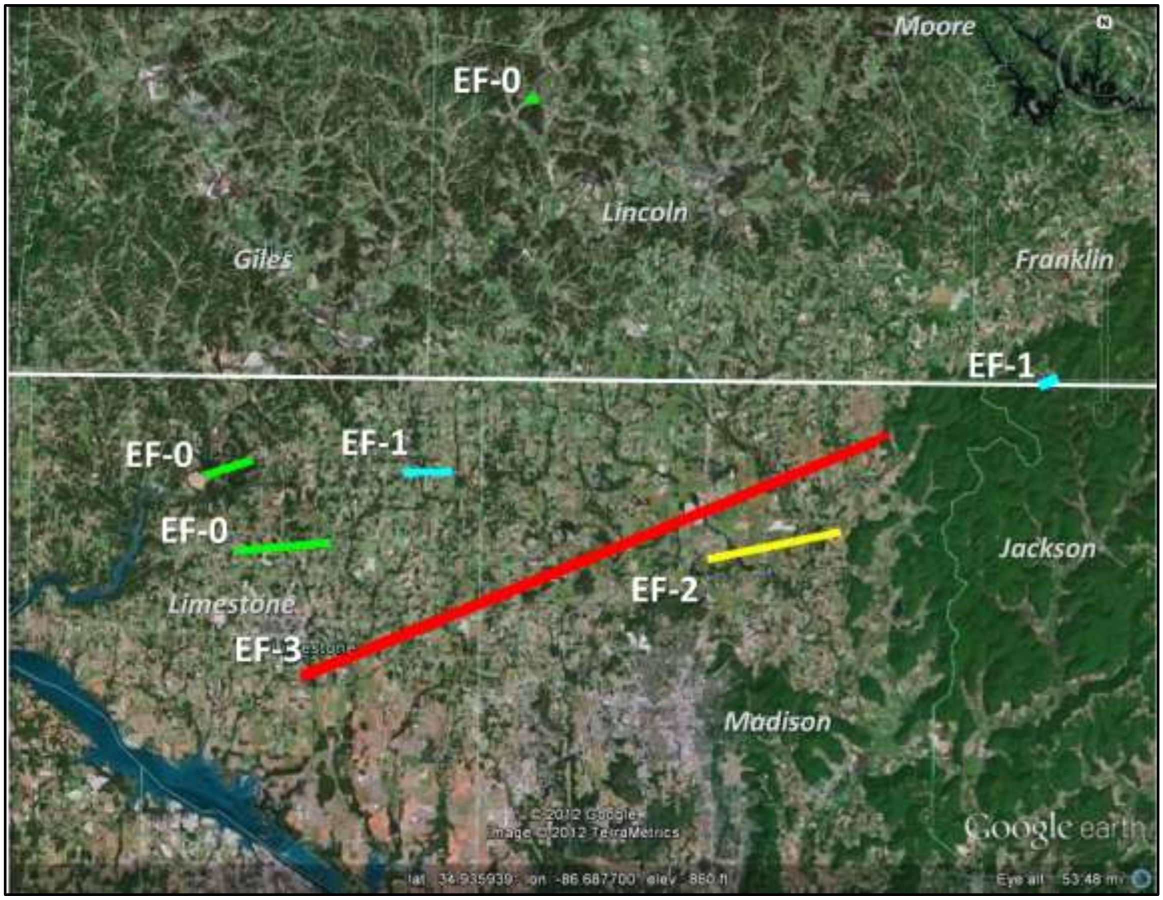

Figure 1: Tornado tracks from 2 March 2012 across northern Alabama and southern Tennessee.

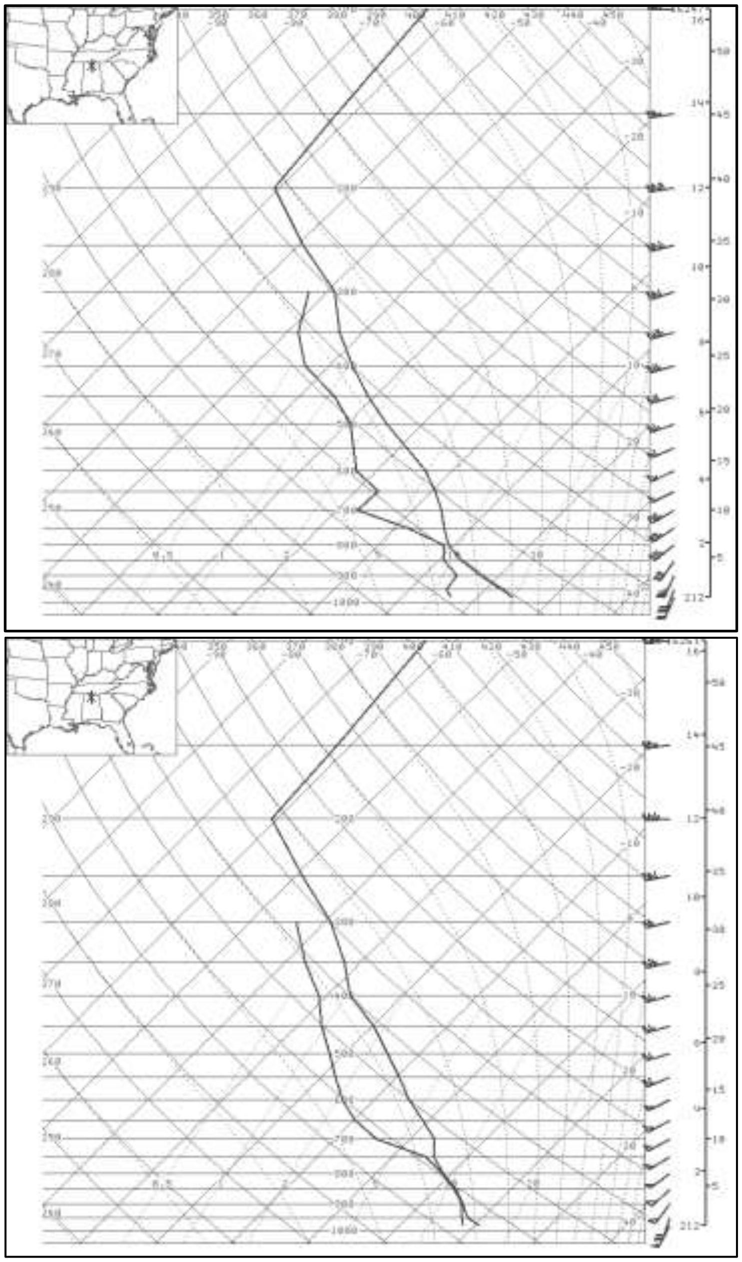

Figure 2a (top) and 2b (bottom): Proximity soundings from the 12-km Rapid Update Cycle (RUC) centered at Huntsville, AL (KHSV) for 1600 UTC (a) and 2000 UTC (b) on 2 March 2012.

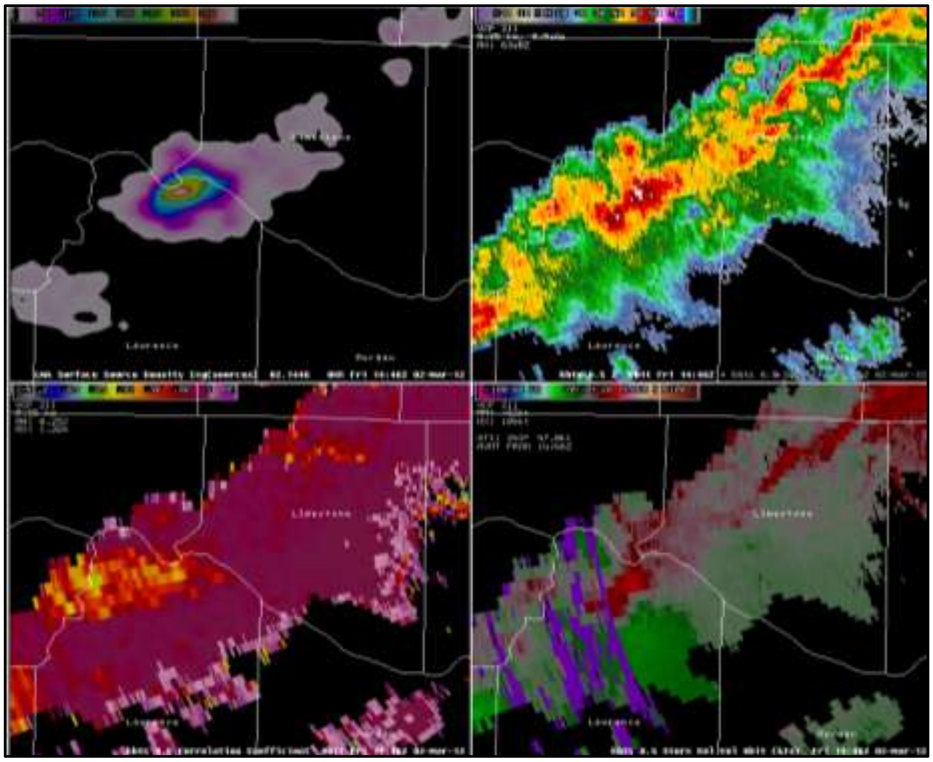

Figure 3: NALMA source density product (top-left) ; KHTX 0.5-degree reflectivity (top-right); KHTX 0.5-degree Storm Relative Velocity (bottom-right); KHTX 0.5-degree Correlation Coefficient (bottom-left), all valid 1446 UTC.

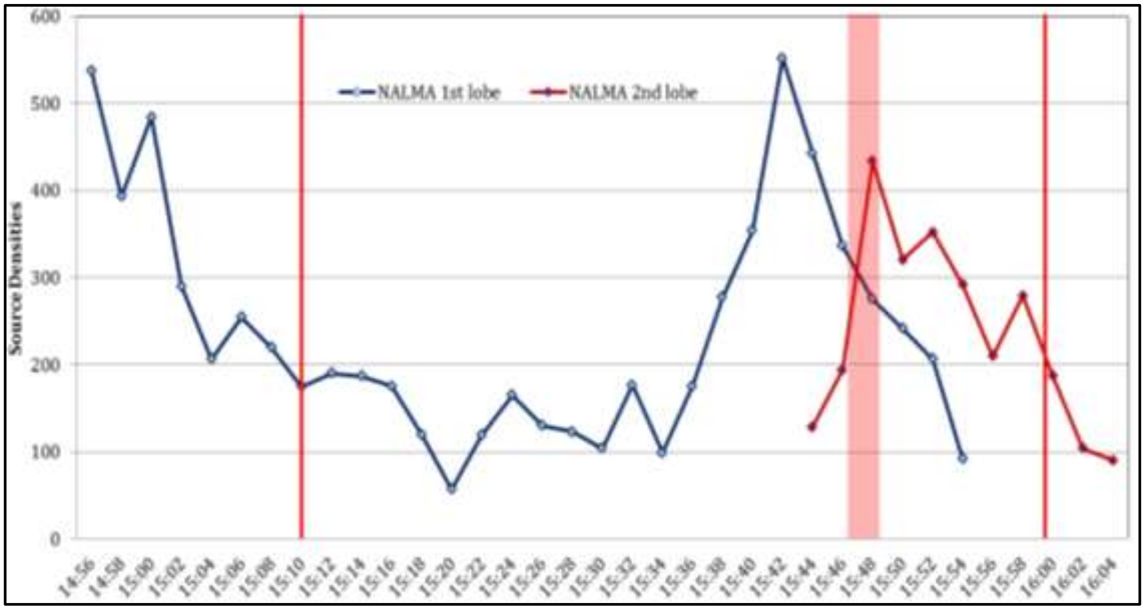

Figure 4: NALMA source density versus time for the EF-3 tornado. Vertical red lines indicate (1) the start time, (2) peak intensity, and (3) end time of the tornado, respectively.

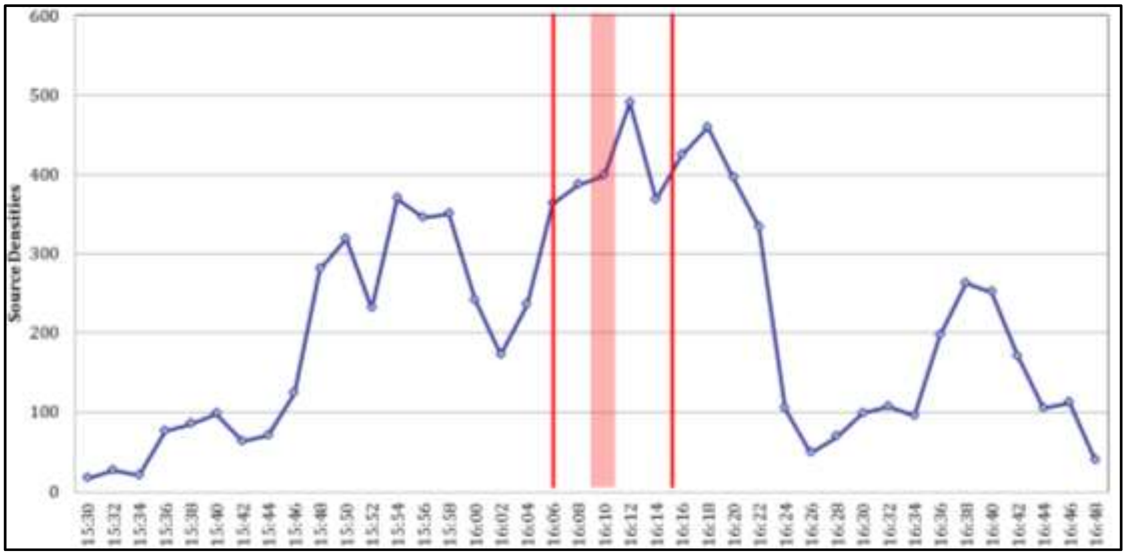

Figure 5: As in Figure 4, except for the EF-2 tornado.

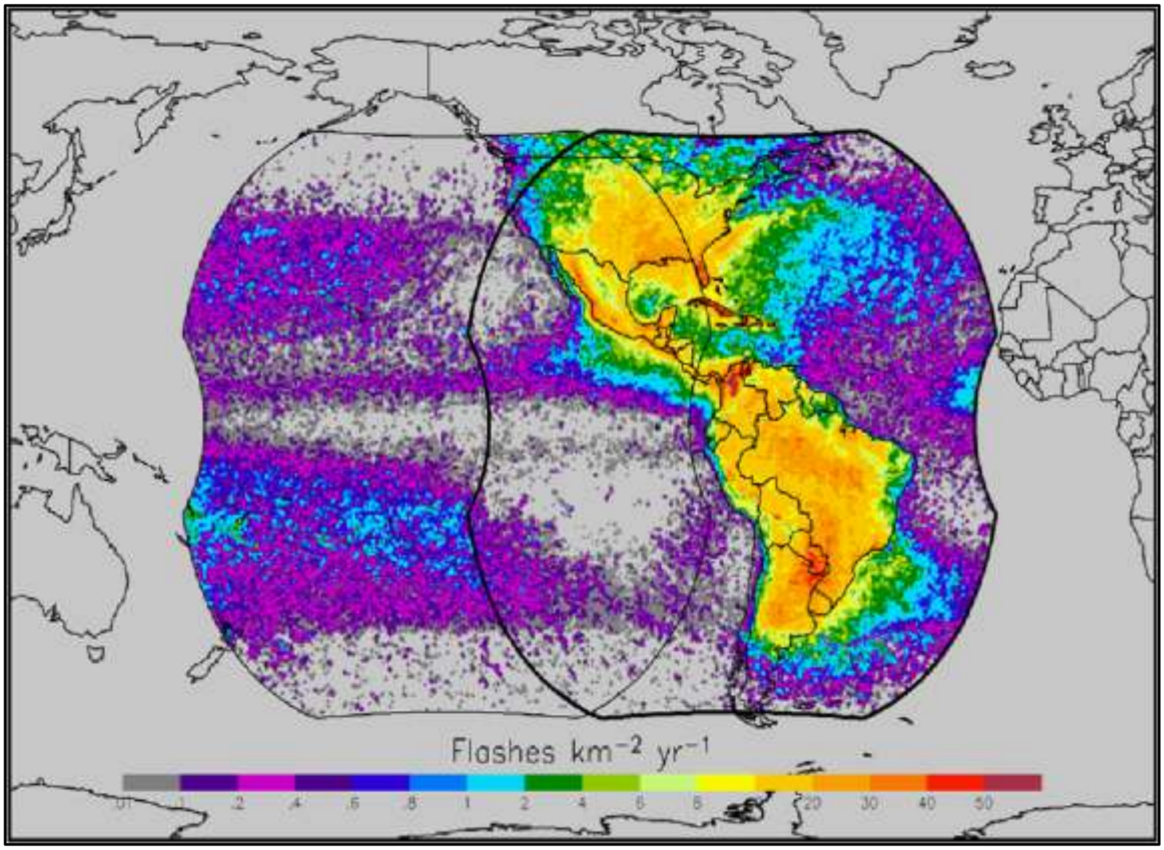

Figure 6: Anticipated domains of the Geostationary Lightning Mapper from the GOES-East and GOES-WEST positions, outlined in black. The background image reflects a lightning climatology derived from the Lightning Imaging Sensor and Optical Transient Detector.

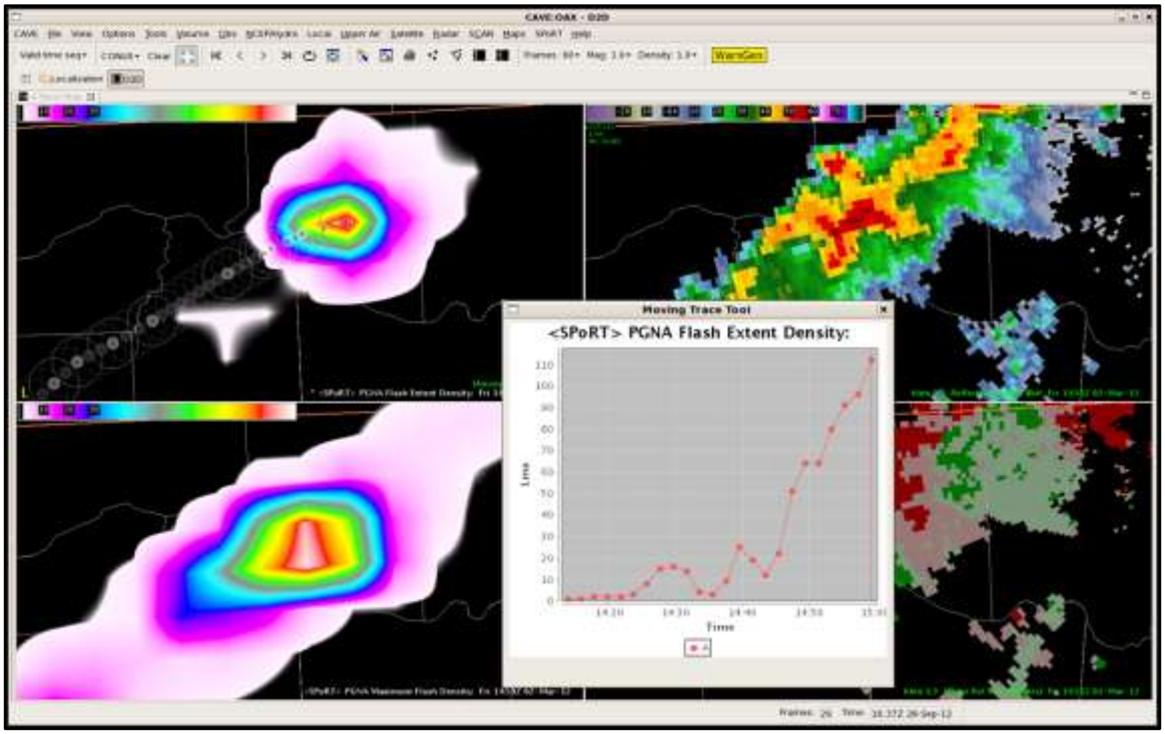

Figure 7: An AWIPS (Advanced Weather Interactive Processing System) 2 "CAVE" (Common AWIPS Visualization Environment) window illustrating total lightning information from the NALMA and the storm-tracking centroid (top-left), KHTX 0.5-degree reflectivity (top-right), KHTX 0.5-degree Storm Relative Velocity (bottom-right), and maximum flash density over 30 minutes (bottom-left). The line graph near center illustrates output from the moving trace tool.